Protistology 17(4): 189–204 (2023) | doi:10.21685/1680-0826-2023-17-4-1

Protistology

ORIGINAL ARTICLE

Diachea racemosa (Myxomycetes = Myxogastrea): a new species with cespitose sporocarps from southern Vietnam and its position within the phylogenetic clade *Diachea* sensu lato (Physarales)

Yuri K. Novozhilov[1,*], Ilya S. Prikhodko[1], Fedor M. Bortnikov[2], Oleg N. Shchepin[1], Anna D. Luptakova[1], Ksenia D. Dobriakova[3], and Thi Ha Giang Pham[4]

[1] *V.L. Komarov Botanical Institute of the Russian Academy of Sciences, 197376 St. Petersburg, Russia*
[2] *Lomonosov Moscow State University, Faculty of Biology, Mycology and Algology Dept., 119234 Moscow, Russia*
[3] *St. Petersburg State University, Faculty of Biology, 199034 St. Petersburg, Russia*
[4] *Joint Vietnam-Russia Tropical Science and Technology Research Centre, Nguyen Van Huyen, Nghia Do, Cau Giay, Hanoi 122100, Vietnam*

| Submitted October 9, 2023 | Accepted November 8, 2023 |

Summary

A new species of dark-spored myxomycetes is described from specimens collected in Bidoup Nui Ba National Park (Dalat Plateau, southern Vietnam) on cushions of mosses covering coarse wood debris of *Quercus* sp. and a log of an indeterminate deciduous tree. Relevant details of morphological characters of the new taxon are provided: shortly ovoid or cylindrical sporocarps assembled in clusters of 0.3–1 cm in diameter and hanging on white or light cream-rose membranous strands of hypothallus; columella membranous and flexuous, pale at the base and dark in the upper part; limeless brown threads of capillitium, spreading from all parts of the columella, slender at the tips; thin membranous silver-metallic iridescent peridium without visible inclusions of lime; free ellipsoid or slightly polygonal large spores covered with rough warts merging into short crests and clusters. Phylogeny reconstruction based on partial sequences of three unlinked genes shows that a new species forms a monophyletic clade with *Diachea cylindrica* (sensu Lado et al., 2022) and occupies position within the clade *Diachea* sensu lato. The genus-level taxonomical classification of some members of this clade is currently uncertain. In this context, the morphology and phylogenetic position of *Paradiachea cylindrica* and *Badhamia lilacina* based on specimens collected in the Russian Far East and the European part of Russia correspondingly are discussed. Decisions that can be made for the taxonomic revision of the genera *Diachea, Paradiachea* and *Scyphium* are summarized.

Key words: Amoebozoa, genome skimming, molecular phylogeny, morphology, small subunit ribosomal RNA, taxonomy, translation elongation factor 1-alpha

https://doi.org/10.21685/1680-0826-2023-17-4-1

***Corresponding author**: Yuri K. Novozhilov; V.L. Komarov Botanical Institute of the Russian Academy of Sciences, Prof. Popov St. 2k, 197376 St. Petersburg, Russia; **yurynovozh1lov@yandex.ru**

Introduction

During intensive field studies on taxonomic and ecological diversity of mycobiota in Vietnam conducted in the frame of the program Ecolan 1.5 of the Joint Russian-Vietnamese Tropical Research and Technological Centre in autumn of 2017 and 2019, we found two large colonies of sporocarps of a dark-spored myxomycete of the subclass Columellomycetidae (Leontyev et al., 2019). Both collections were found in mountain deciduous monsoon tropical forests in the Bidoup Nui Ba National Park (BNB) of southern Vietnam (Lam Dong Province) in adjacent localities. In both cases, the microhabitat was moist moss tussocks covering the bark of dead trunks of deciduous trees.

The general appearance of fruiting bodies resembled the limeless sporocarps of *Badhamia utricularis* (Bull.) Berk. Moreover, habitats associated with mosses were also characteristic of some representatives of the genus *Badhamia* (Ing, 1994). For these reasons, we tentatively identified these specimens as *Badhamia* sp. (Novozhilov et al., 2020).

The reconstruction of the four-gene phylogeny of Physarales showed that this taxon occupied position within the clade *Diachea* sensu lato in the phylogenetic tree (García-Martín et al., 2023), which also included *Diachea cylindrica* Bilgram (= *Paradiachea cylindrica* (Bilgram) Hertel ex H. Neubert, Nowotny and K. Baumann) sensu Lado et al. (2022) and García-Martín et al. (2023). Unfortunately, a confusion was introduced by publication of nrSSU and EF1α sequences of one of the two specimens of *Badhamia* sp. from Vietnam (LE 317581) under a wrong name *Badhamia lilacina* (Fr.) Rostaf. (GenBank MW692988 and MW701625; Shchepin et al., 2021; García-Martín et al., 2023).

In this regard, and to avoid further confusion, we present here the illustrated morphological data and a new three-gene phylogenetic tree, which includes specimens of *Craterium lilacinum* (Fr.) Massee (≡ *Badhamia lilacina*) and *P. cylindrica* from the European part of Russia and Russian Far East, respectively, with the morphology typical for these species, and shows the phylogenetic position of the two specimens of the new species *Diachea racemosa*. We provide a detailed morphological description of the new species and summarize decisions that can be made for the taxonomic revision of the genera *Paradiachea* Hertel. and *Scyphium* Rostaf.

Material and methods

Material studied

The specimens considered herein were collected at two localities of BNB centred in the Bi Doup mountain range (12°08′ N, 108°40′ E) in the southern Annamite Mountains, on the Dalat Plateau. The topography of this area is dominated by a range of high mountains, including Bidoup Mt. (2,287 m a.s.l.) and Gia Rich Mt. (1,922 m a.s.l.). The rainy season in the region extends from May to October, and the dry season encompasses the period from December to April. The predominant vegetation is a montane evergreen forest, with small patches of coniferous forest and middle mountain mixed broadleaved deciduous polydominant forest including members of Fagaceae and Magnoliaceae along with *Pinus kesiya* Royle ex Gordon, *P. dalatensis* Ferré, and *P. krempfii* Lecomte. Detailed information about vegetation, climate and landscape of BNB is given in Novozhilov et al. (2020). The two specimens described in this paper were recorded during two different field surveys in November 2017 and October 2019.

The localities for all collections were georeferenced with a portable GPS device (WGS 84 mapping data). Voucher specimens are deposited in the myxomycete collection of the mycological herbarium in the Komarov Botanical Institute, Laboratory of Systematics and Geography of Fungi (LE).

Morphological analyses

Air-dried sporocarps were studied with an Axio Imager A1 (Carl Zeiss AG, Germany) light microscope (LM) with differential interference contrast (DIC), a Stemi 2000 dissecting microscope (DM), a Zeiss motorized stereomicroscope ZEISS Axio Zoom.V16, and a JSM-6390LA (JEOL, Japan) scanning electron microscope (SEM) at the Core Facility Center of the Komarov Botanical Institute of the Russian Academy of Sciences. *Paradiachea cylindrica* and *Craterium lilacinum* (≡ *B. lilacina*) were studied with scanning electron microscopes CamScan S-2 (Cambridge Instruments, UK) and Quattro S (Thermo Fisher Scientific, USA) in the Interdepartmental Laboratory of Electron Microscopy at the Faculty of Biology, MSU. For microscopy, sporocarps were preserved as permanent sli-

des in polyvinyl-lactophenol. Microscopic measurements were made using Zeiss Zen 3.2 software (free license, blue edition). The average spore diameter (including spore ornamentation) was calculated from 50 spores measured for each collection. Specimens for SEM were mounted on copper stubs with a double-sided tape or thin layer of nail polish and sputter-coated with gold.

DNA extraction

Extraction of genomic DNA for Sanger sequencing was performed from matured air-dried sporophores without a trace of fungal contamination. Approximately 2-5 sporophores were placed in 2 ml plastic tubes with screw caps. Ceramic beads 3 mm in diameter were added, tubes were frozen at -20 °C for at least 30 min and samples were finally homogenized in a Bioprep-24 homogenizer (Hangzhou Allsheng Instruments, China) with three cycles of 10 seconds at a speed of 6 m/sec, with intervals of 5 sec. DNA was extracted with a PhytoSorb kit (Sintol, Russia) according to the manufacturer's protocol with minor modifications: spore homogenate was eluted with 450 µl of extraction buffer; lysis buffer was added without preliminary precipitation step and supernatant transfer into a new sterile tube; final elution volume was 80-100 µl.

DNA amplification and Sanger sequencing

Since nucleotide sequences previously published (GenBank MW692988 and MW701625; Shchepin et al., 2021) from the type specimen of the new species showed the highest affinity to *Diachea cylindrica* (García-Martín et al., 2023), we decided to obtain three unlinked genetic markers from this species for phylogeny reconstruction. A fragment of approximately 550-800 base pairs from the 5' end of the nuclear 18S rDNA gene (nrSSU) that is free of introns was obtained with forward primer S2 and reverse primer SSU_rev (Fiore-Donno et al., 2008; Prikhodko et al., 2023a). Fragments of the protein-coding gene for the translation elongation factor 1-alpha (EF1α) were obtained using the PB1F/PB1R primer pair (Novozhilov et al., 2013) and, in some cases, expanded with fragments obtained using a set of primers for a semi-nested PCR EF03(EF04)/KEF_R3 (Wrigley de Basanta et al., 2017; Ronikier et al., 2020). Fragments of mitochondrial 16S rDNA (mtSSU) were obtained using the Kmit_F/Kmit_R primer pair (Lado et al., 2022). Additionally, a fragment of mitochondrial cytochrome c oxidase I gene (COI) was obtained for the holotype of the new species using primers COIF1/COIR1 (Feng and Schnittler, 2015). Composition of PCR mixtures, sample preparation and sequencing parameters were described in detail in Prikhodko et al. (2023a, b) and Bortnikov et al. (2023).

Low-pass genome sequencing

To verify the quality of the Sanger sequencing and to obtain longer sequences of marker genes for future studies, we separately performed DNA isolation and low-pass genome sequencing of samples belonging to key species of the genus *Diachea* sensu García-Martín et al. (2023) (*Diachea bulbillosa* (Berk.et Broome) Lister, *D. dictyospora* (Rostaf.) J.M. García-Martín, J.C. Zamora et Lado, *D. leucopodia* (Bull.) Rostaf., *D. silvaepluvialis* M.L. Farr), *Paradiachea cylindrica,* and *Badhamia lilacina*. For this purpose, we used ExtractDNA Blood and Cells (Evrogen, Russia) spin column extraction kit according to the protocol we applied earlier for *Kelleromyxa fimicola* (Dearn. et Bisby) Eliasson (Prikhodko et al., 2023b).

The spectral characteristics and DNA content of the DNA extracts were measured with an Implen P300 nanophotometer (Implen, USA). Further DNA quality control, library preparation and shot-gun whole-genome sequencing were performed by a third-party organization (Institute of Genomic Analysis, Moscow, Russia). DNA was fragmented using Covaris ME220 (Covaris, USA) to achieve fragment length distribution peak in range 250-320 bp, then DNA library was prepared using MGIEasy Universal DNA Library Prep (MGITech, China). Sequencing with target coverage of the nuclear genome 2X was performed on DNBSeq 400 (MGITech, China) using DNBSEQ-G400RS High-throughput Sequencing Set (FCL PE150) according to manufacturer's instructions. The resulting paired-end reads of 150 bp length were assembled in contigs using SPAdes 3.15.4 (Prjibelski et al., 2020) with a --careful flag for a more thorough error correction. Summary statistics were calculated using QUAST 5.2.0 (Mikheenko et al., 2018). Candidate sequences for orthologs of nrSSU, EF1α and mtSSU were identified using local discontinuous MegaBLAST search across the obtained contigs against a custom-made reference BLAST database.

Sequence alignment and phylogenetic analyses

nrSSU, EF1α and mtSSU sequences were combined in three multiple alignments in Unipro UGENE (Okonechnikov et al., 2012) and aligned using MAFFT online service (Katoh and Standley, 2013; Katoh et al., 2019) with E-INS-I option for nrSSU and mtSSU or G-INS-i option with default gap penalties for EF1a sequences. After manual editing and primer trimming, three sets of nucleotide sequences were merged into a single alignment using SequenceMatrix 1.9 (Vaidya et al., 2011). The exon parts of the EF1α sequences were determined according to the sequences from *Collaria nigricapillitia* (Nann.-Bremek. and Bozonnet) Lado (GenBank AY643818; Fiore-Donno et al., 2005; Fiore-Donno et al., 2010) and *Echinostelium bisporum* (L.S. Olive et Stoian.) K.D. Whitney et L.S. Olive (GenBank MH814572; Fiore-Donno et al., 2019).

The concatenated dataset consisted of four partitions. The nrSSU was analyzed as an entire partition between the SSU and SSU_rev primer landing sites. The hypervariable mtSSU fragment at positions 2450-2632 was cut off for the analysis (see Supplementary Files S1, S2). Two separate partitions were defined for the EF1α sequences: the first and second positions of each codon were analyzed separately from the third positions, as was done in Prikhodko et al. (2023b).

The final alignment consists of 144 sequences (142 nrSSU sequences, 134 EF1α sequences, and 117 mtSSU sequences, respectively) with 2721 sites, 1794 distinct patterns, 288 singleton sites and 1205 non-informative (constant) sites in total. Maximum likelihood (ML) analyses were performed using IQ-TREE 1.6.12 (the last stable release; Nguyen et al., 2015) launched on a local machine. The TIM2e+R5 and GTR+F+I+G4 models were selected for the nrSSU and mtSSU partitions, respectively, according to the ModelFinder tool implemented in the program (Kalyaanamoorthy et al., 2017). JC+I+G4 and GTR+F+G4 models were selected for the first two and the third positions of each codon in EF1α partitions, respectively. Ultrafast bootstrap analysis with one thousand replicates (Hoang et al., 2018) was performed to obtain confidence values for the branches. Bayesian analysis was performed with the same dataset using mrBayes 3.2.7a (Huelsenbeck and Ronquist, 2001) run on CIPRES Science Gateway (Miller et al., 2010); the GTR+G+I model was applied. The phylogenetic analysis was run four times as four separate chains for 10 million generations (sampling every 1000). The convergence of MCMCMC was estimated using TRACER 1.7.2 (Rambaut et al., 2018); based on the estimates by TRACER, the first 2 million generations were discarded as burn-in. Posterior probabilities (PP) of splits were exported to the best-scoring ML-tree. Phylogenetic tree with combined supports was visualized using FigTree 1.4.4 and edited using CorelDRAW 24.0.

Results

Low-pass genome sequencing data analysis

The search for orthologs of the three target genomic regions among the contigs resulting from the assembly of the low-pass genome sequencing (genome skimming) data yielded complete or nearly complete sequences of nrSSU, mtSSU and EF1α for all 6 specimens (Table 1). The overlapping fragments of sequences obtained by Sanger sequencing and high-throughput sequencing matched completely.

Phylogeny

A total of 101 new nucleotide sequences were generated for this study, including close to complete sequences of nuclear 18S rDNA (nrSSU), nuclear translation elongation factor 1-alpha (EF1α), mitochondrial 16S rDNA gene (mtSSU), and mitochondrial cytochrome c oxidase I (COI).

The resulting three-gene phylogeny is shown in Fig 1. The tree is rooted with *Barbeyella minutissima* Meyl. and *Echinostelium bisporum* (Echinosteliales) followed by *Meriderma species* (Meridermatales) with unresolved branching. The rest of the tree generally repeats the topologies demonstrated in the two-gene (Novozhilov et al., 2022; Prikhodko et al., 2023b), three-gene (Prikhodko et al., 2023a) and four-gene (García-Martín et al., 2023) phylogenies: species of the genus *Lamproderma* (Lamprodermataceae), including the type species *L. columbinum* (Pers.) Rostaf., occupy a basal position relative to the families Didymiaceae sensu lato and Physaraceae sensu stricto within the clade corresponding to the order Physarales sensu lato (Fig. 1). Most genera within the order Physarales form monophyletic clades with branch supports greater than 90/0.9. However, the genus *Diachea* (sensu García-Martín et al., 2023) receives low

Table 1. Sequencing depth and coverage of the three target genes for the samples analysed using low-pass genome sequencing.

Species	Voucher	Depth (Million bp)	Contigs	nrSSU coverage	EF1A coverage	mtSSU coverage
Diachea dictyospora	LE286398	1407.67	380740	186	1	1268
Diachea bulbillosa	LE297619	611.1926	218485	7	1	64
Craterium lilacinum (≡ *Badhamia lilacina*)	LE319161	750.47	266008	230	1	236
Diachea leucopodia	LE328364	922.1	200736	45	2	720
Diachea silvaepluvialis	MYX11337	1749.87	270103	171	4	1564
Paradiachea cylindrica	MYX11357	1324.26	174392	345	3	1267

support in the ML analysis (UBS/PP = 83/1), and the genus *Diderma* represented by six species splits into two clades with unresolved position.

The *Diachea* clade (Fig. 2) includes all species of the clade 3 in García-Martín et al. (2023). It is extended by additional sequences, including nine specimens of *Badhamia lilacina* in a fully supported monophyletic clade "Scyphium" and two specimens of *Diderma cor-rubrum* T. Macbr. forming a well-supported clade with *Diachea subsessilis* (UBS/PP = 87/0.99). Two specimens from Vietnam, originally identified as *Badhamia* sp. (Novozhilov et al., 2020) and later erroneously labelled as *B. lilacina* (Shchepin et al., 2021; García-Martín et al., 2023), form a monophyletic clade with *Diachea cylindrica* sensu Lado et al. (2022). However, the specimen determined by us as *Paradiachea cylindrica* (≡ *D. cylindrica*) sensu stricto, for which both Sanger sequences and genomic data were obtained, occupies a basal position in Didymiaceae sensu lato (UBS/PP = 94/0.7). This specimen shows a large number of mismatches in EF1α and mtSSU sequences and unique long insertions in the nrSSU fragment when compared with two specimens of *D. cylindrica* sensu Lado et al. (2022).

Morphology and taxonomy

Craterium lilacinum (Fr.) Massee, Monogr. Myxogastr. 271 (1892), Fig. 3; ≡ *Badhamia lilacina* (Fr.) Rostaf. Sluzowce monogr. 145 (1874).

Sporocarps — sessile sporangia or subsessile sporangia with stalk-like base up to 100 μm, crowded to overlapping, globose, ovoid to shortly cylindrical (Fig. 3, C). Sporotheca 300–600 (–750) μm high, 300–650 μm wide. Hypothallus thin, membranous, inconspicuous to pale brown. Peridium double, consisting of two closely appressed layers. Inner layer thin, membranous, hyaline. Outer layer thick, densely calcified, dirty grey to pale pinkish grey (Fig. 3, D). Capillitium badhamioid, reticulate, almost entirely calcareous, white to flesh-colored, sometimes forming a pseudocolumella in the center of the sporotheca (Fig. 3, D). Spores dark brown to black in mass (Fig. 3, D), dark purple brown in transmitted light (Fig. 3, E), ornamented with ridges forming a very incomplete reticulum (Fig. 3, F), (13.5–) 14.0–15.0 (–15.8) μm in diameter (Mean = 14.50, SD = 0.45, n = 50). Plasmodium is yellow before sporocarp formation (Fig. 3, B). Habitat: on living plants and mosses in bogs (Fig. 3, A, B).

Examined specimen: RUSSIA, Murmansk region, the vicinity of the Tietta research station, sphagnum bog with *Pinus sylvestris* L., on living grass and mosses, 67.600738°N, 32.996322°E, 25 VIII 2023, leg. Filippova A.V. and Bortnikov F.M., LE F-348758.

For other specimens included in the phylogenetic analysis and illustrated below, see Supplementary Table S1.

Diachea racemosa **sp. nov.** Novozh., Bortnikov, Prikhodko et Shchepin, Figs 4, 5.

MycoBank: MB#849476, **GenBank**: nrSSU – MW692988; EF1a – OR759917; mtSSU – OR769424; COI – OR778615

Etymology: from latin racemosus – clustering, refers to the shape of sporocarp colonies.

Description: Sporocarps aggregated into clusters 1.5–10 mm in diameter that include up to 100 sporangia, pendent on thin, strand-like white or light cream-rose membranous hypothallus (Fig. 4, B–E). Sporotheca of a sporangium ovoid or obpyriform, 300–500 μm in diameter (Fig. 4, D, E). Peridium membranous, thin, reddish grey to dark reddish grey and metallic iridescent under a dis-

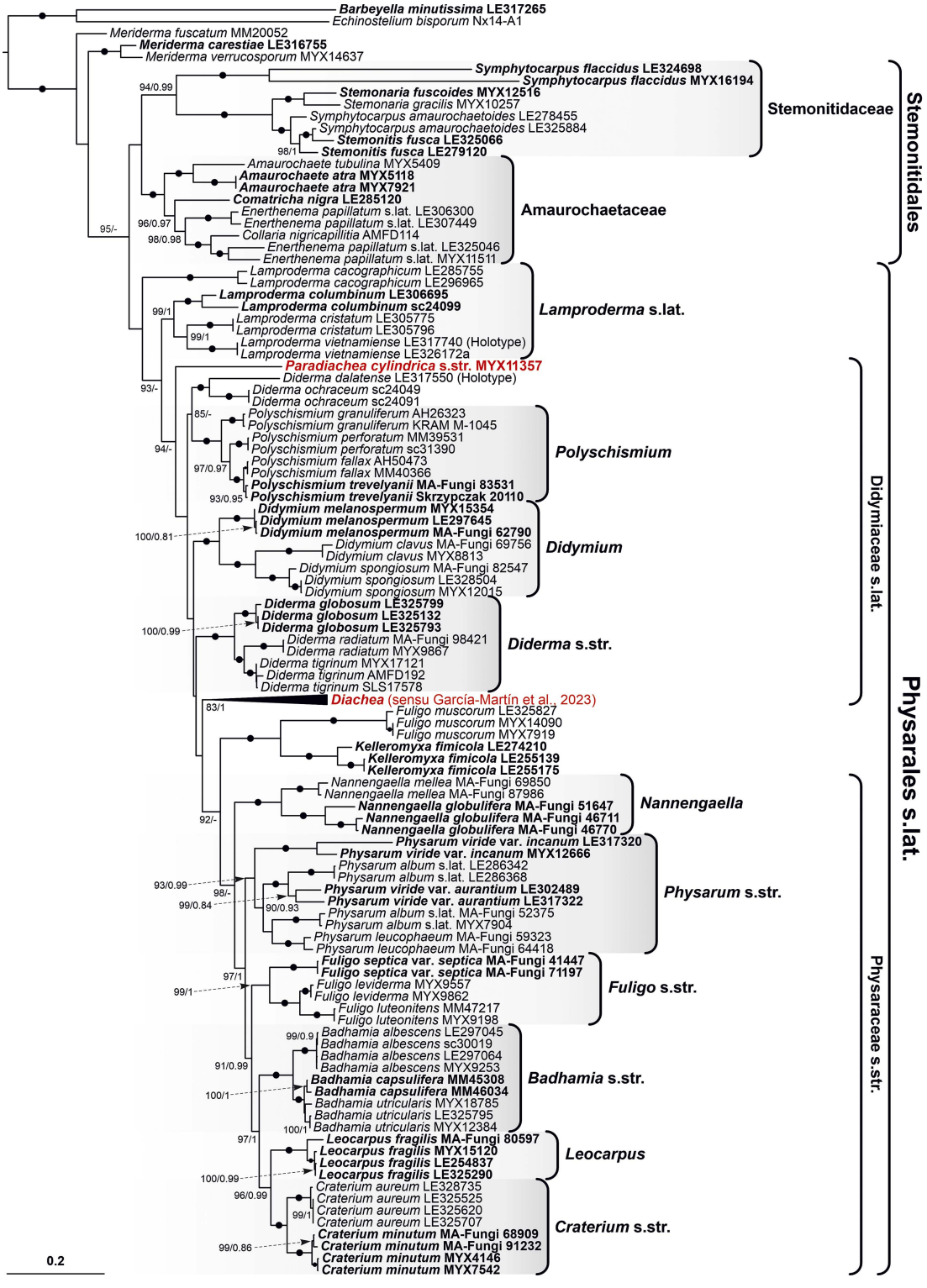

Fig. 1. Maximum-likelihood phylogenetic tree obtained from concatenated nrSSU, mtSSU and EF1α sequences. Bold font indicates type species of genera. Branch supports below UBS 80 or PP 0.8 are not shown; black dots indicate maximum supports in both analyses (UBS/PP = 100/1); scale bar represents the mean number of nucleotide substitutions per site. The clade "*Diachea* (sensu García-Martín et al., 2023)" is collapsed for representation in a separate illustration. The nomenclature used in the tree is checked against the current version of the nomenclature database of Lado (2005–2023).

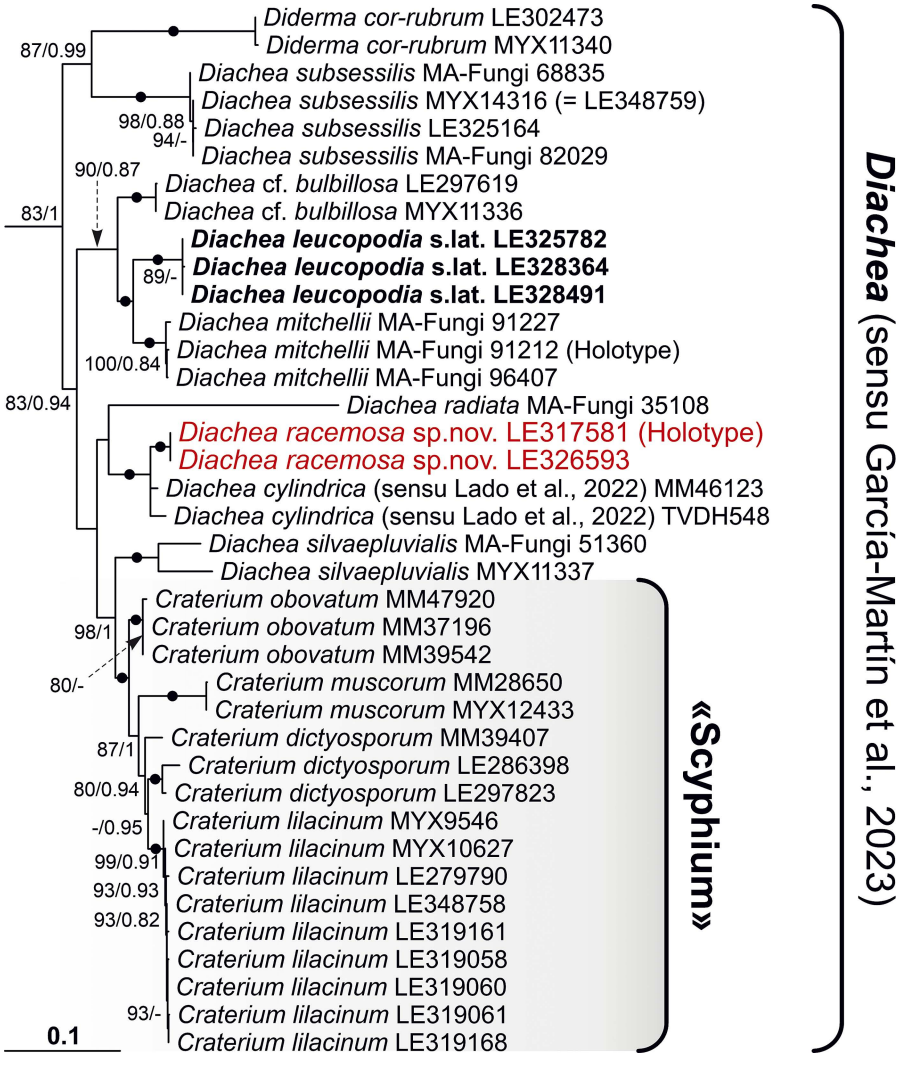

Fig. 2. Detailed representation of the clade "*Diachea* (sensu García-Martín et al., 2023)". Bold font indicates the type species *D. leucopodia*. Branch supports below UBS 80 or PP 0.8 are not shown; black dots indicate maximum supports in both analyses (UBS/PP = 100/1); scale bar represents the mean number of nucleotide substitutions per site. The illustration includes species names prior to the nomenclatural revision by *García-Martín* et al. (2023).

secting microscope (Fig. 4, D–F), without visible inclusions of lime, partially evanescent (Fig. 4, F). Columella arising from the base of sporotheca and almost reaching the apex of the sporangium, slightly fibrous, sometimes distinctly membranous, flexuous, limeless, pale at the base and dark in the upper part. Capillitium scanty, consisting of limeless, brownish to black threads, arising from all parts of the columella, occasionally branching and anastomosing, slender at the tips. Spores dark greyish reddish brown in mass, light reddish brown to moderate reddish brown in transmitted light (Fig. 5, A), subglobose, ellipsoid, ovoid or slightly polygonal, coarsely verrucose, (14.7–) 15.6–17.3 (–18.8) × (15.7–) 16.5–19.0 (–24.1) µm (n = 100), with the surface ornamentation formed by rough warts merging into short crests and clusters (Fig. 5, A–C). Plasmodium unknown.

Holotype: Vietnam, Lam Dong Province, Southern Annamite Mountains, the Dalat Plateau, Bidoup Nui Ba National Park, Giang Ly Ranger Station, 12.1869°N, 108.6756°E, elevation ca 1440 m, middle mountain broadleaved deciduous polydominant tropical forest dominated by *Lithocarpus* sp., *Quercus* sp., and *Castanopsis* spp., on mosses and liverworts covering upper branches of a recently broken tree of *Quercus* sp., 14 XII 2017, leg. Novozhilov Yu. K., LE 317581.

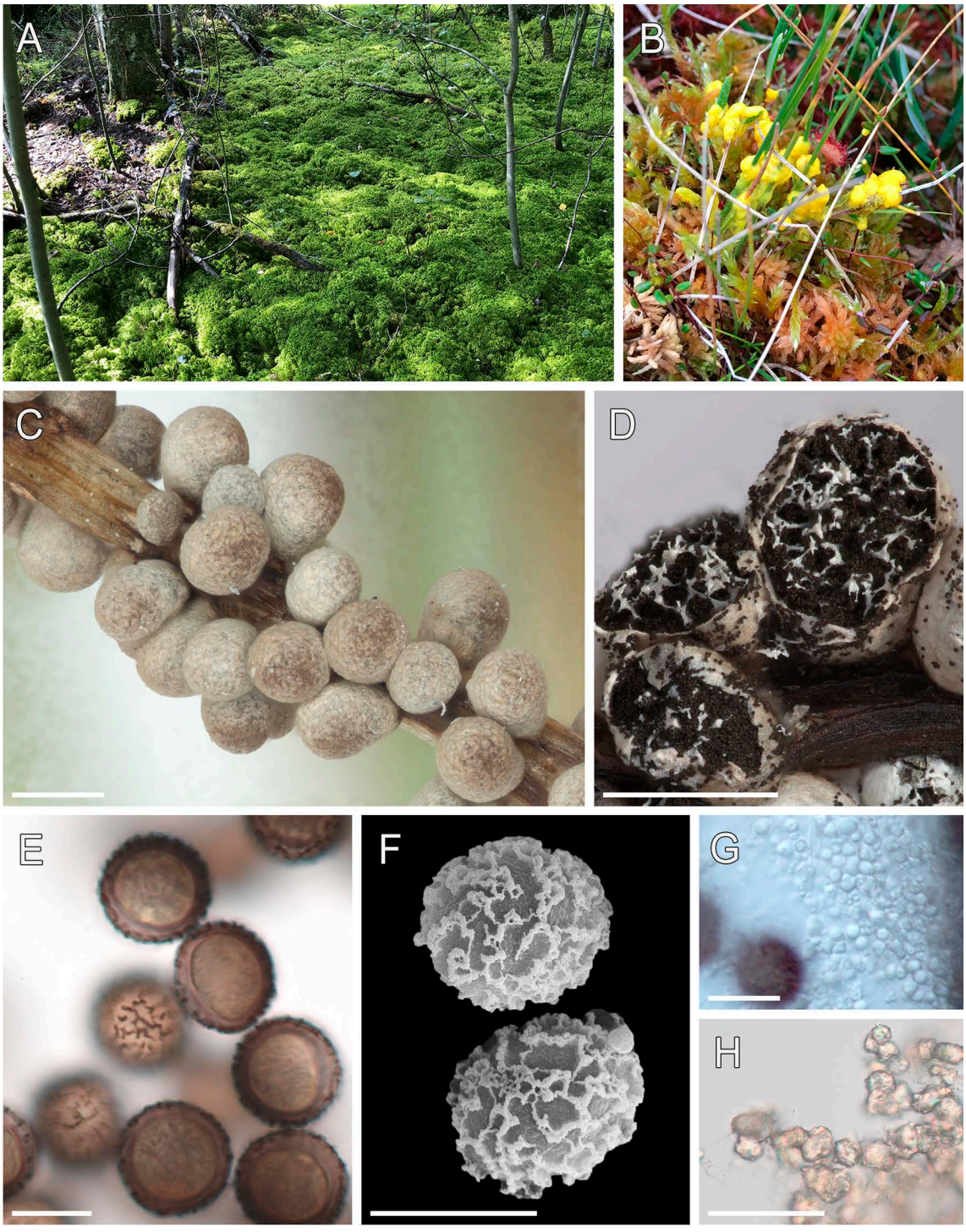

Fig. 3. A–G — *Craterium lilacinum* (≡ *Badhamia lilacina*) (B, C, E, F — LE F-348758, D, G — LE 319161, F — from LE 319060). A — Habitat in the Central Forest Reserve (specimens LE 319058, LE 319060 and LE 319061); B — plasmodium on the surface of grass and mosses in the bog; C — sessile matured sporangia; D — disrupted sporangium with badhamioid capillitium; E — spores (LM); F — spores (SEM); G — lime granules; H — *Craterium dictyosporum* (LE 286398): prismatic and rhombohedral crystals from stalk (LM). Scale bars: C, D = 500 μm; H = 50 μm; E, F, G = 10 μm.

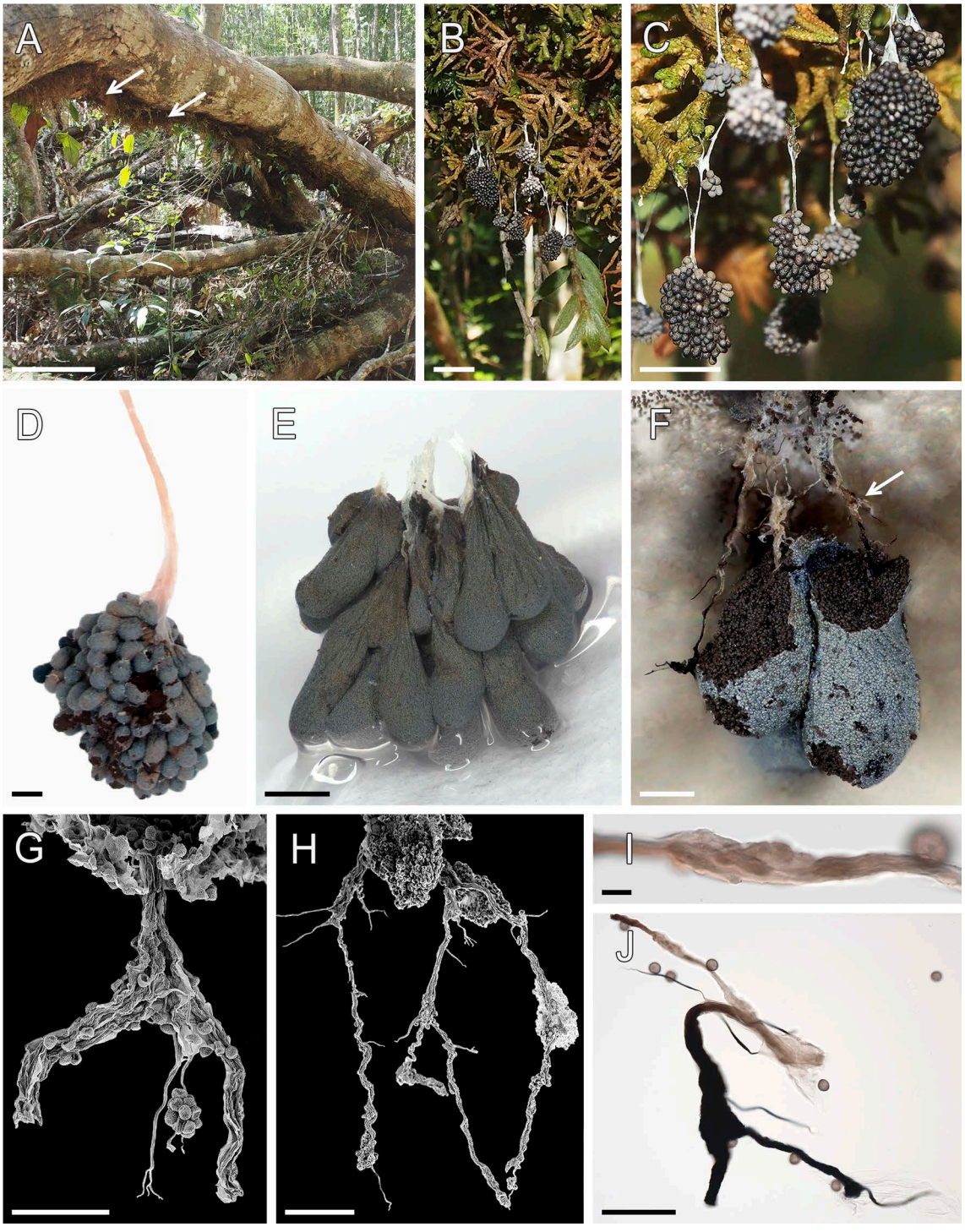

Fig. 4. *Diachea racemosa* sp. nov. (A–D, F–H —holotype LE 317581, E, I, J — paratype LE 326593). A — Habitat of the type specimen (arrows show the position of sporocarps); B, C — colony of sporocarps on bryophytes, as seen in the field; D, E — parts of a colony of sporocarps as seen under a dissecting microscope (DM); F— opened sporocarps with membranous peridium and irregular, limeless columella (DM), *arrow* shows the position of columella; G–J— columella and capillitium (G, H — SEM, I, J — LM). Scale bars: A = 50 cm; B, C = 1 cm; D, E = 500 μm; F, H= 200 μm; G, J = 100 μm; I = 10 μm.

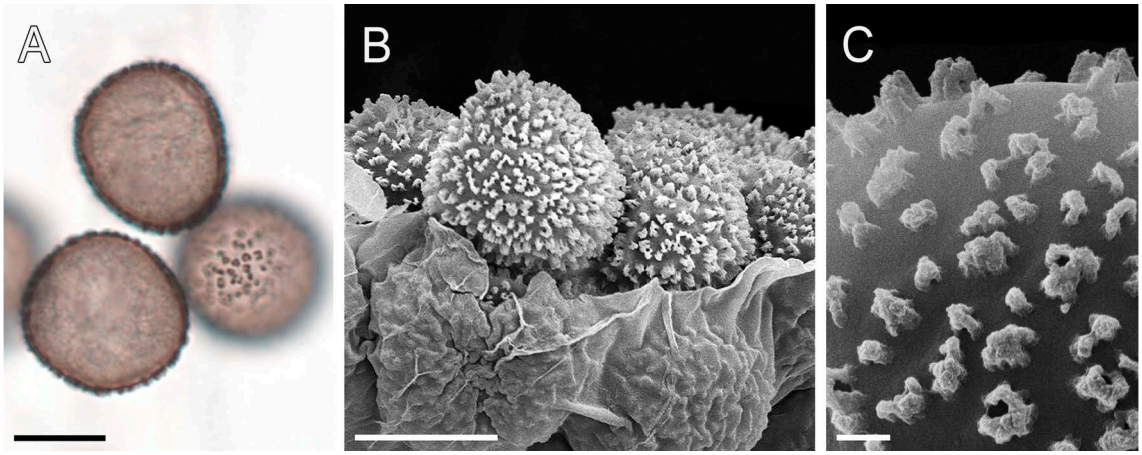

Fig. 5. *Diachea racemosa* sp. nov. (holotype LE 317581). A — Spores (LM), B — peridium and spores (SEM), C — spore ornamentation (SEM). Scale bars: A, B = 10 μm; C = 1 μm.

Paratype: Vietnam, Lam Dong Province, Southern Annamite Mountains, the Dalat Plateau, Bidoup Nui Ba National Park, Giang Ly Ranger Station, 12.1872°N, 108.6741°E, elevation ca 1540 m, mountain broadleaved deciduous tropical forest dominated by *Lithocarpus* sp., *Quercus* sp., and *Castanopsis* spp., on mosses and liverworts covering a log of an undetermined deciduous tree, 29 X 2019, leg. Novozhilov Yu.K., Shchepin O.N, LE 326593.

Distribution: *Diachea racemosa* is currently known only from two localities in Vietnam.

Note: The most distinctive and unique characters of *D. racemosa* are the habit of sporocarps aggregated into clusters 1.5–10 mm in diameter, consisting of 5–100 sporangia, pendent on thin, strand-like white or light cream-rose membranous hypothallus and membranous, flexuous, limeless columella. In addition, free ellipsoid, ovoid or polygonal spores about 15–24 μm in diameter, covered with rough warts merging into short crests and clusters are other key characters of this new species. None of the known species of Physarales has the same combination of characters.

The two *Diachea racemosa* specimens have identical morphology. Paratype LE 326593 has slightly smaller spores that are also slightly more regular in shape (length/width ratio = 1.07 vs 1.10). Spore sizes: LE 317581: (16.2–) 16.9–19.5 (–24.1) (Mean = 18.21, SD = 1.28, n = 50) × (14.7–) 15.7–17.4 (–18.8) (Mean = 16.54, SD = 0.87, n = 50); LE 326593: (15.7–) 16.3–18.4 (–21.4) (Mean = 17.35, SD = 1.03, n = 50) × (14.7–) 15.5–17.1 (–18.8) (Mean = 16.29, SD = 0.82, n = 50).

Paradiachea cylindrica (Bilgram) Hertel ex H. Neubert, Nowotny et K. Baumann, Fig. 6; ≡ *Diachea cylindrica* Bilgram, Proc. Acad. Nat. Sci. Philadelphia 57:524 (1905)

GenBank: SSU – OR769382; EF1a – OR759927; mtSSU – OR769460

Description: Sporangia sessile on a narrowed base, gregarious to crowded, cylindrical with obtuse apex, slightly tapering upwards (Fig. 6, A, B), 1.0–1.8 mm high, 0.50–0.65 mm wide, brownish grey, bronze or golden. Hypothallus very thin, membranous, whitish to brownish. Peridium membranous, iridescent with golden, blue and violet tints, not adhering to the capillitium (Fig. 6, A–C). Columella arising from the base and almost reaching the apex of the sporangium, rather variable, sometimes almost entrely hyaline, sometimes almost entirely light brown except in the lower part, irregular, formed of membranous extensions, rarely more or less regular in the lower half, completely limeless (Fig. 6, C, D, E, G). Capillitium brownish, arising from the columella, branching and anastomosing, with many membranous extensions, denser at the periphery, with pale tips (Fig. 6, C, D). Spores dark brown in mass, pale brown to grey brownish in transmitted light, (12.5–) 13.2–14.2 (–14.6) μm in diameter including ornamentation (Mean = 13.69, SD = 0.49, n = 50), reticulate. Reticulum very uneven, with meshes of different sizes; the ridges forming the reticulum are inaccurate, curved, wider and darker in some places, sometimes the thickening of ridges resembles warts, but there are no truly isolated warts, the height of the ornamentation is 0.7–1.0 μm (Fig. 6, F). Under SEM, the ridges are solid (Fig. 6, H, I), not resembling arched bridges. Plasmodium presumably whitish.

Examined specimen: Russia, Primorsky Krai,

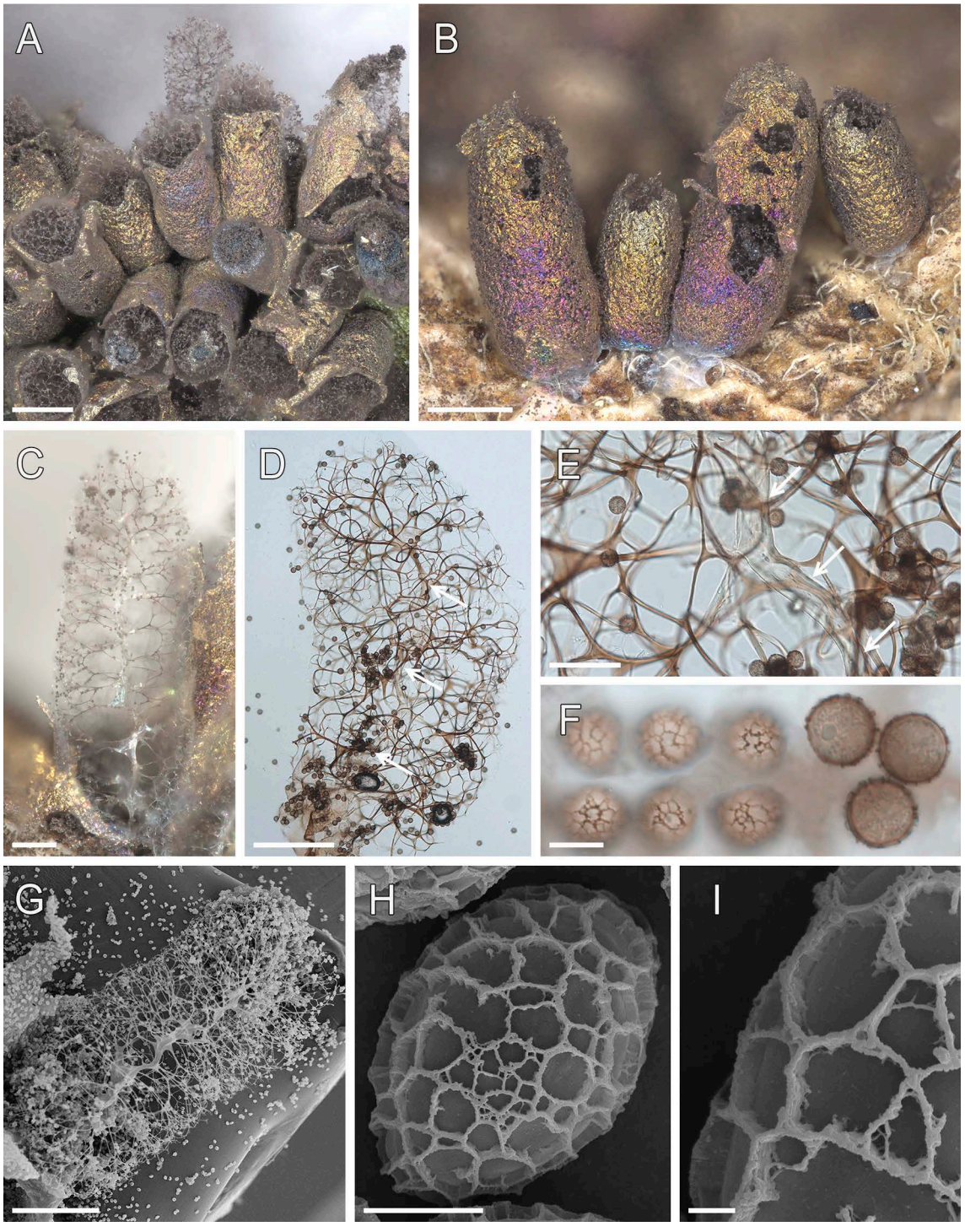

Fig. 6. *Paradiachea cylindrica* (MYX 11357 = LE 328189). A, B — Sporangia; C — sporangium without spores; irregular membranous columella and capillitium branching type are visible; D, E — sporangium (LM), *arrows* point to the columella; F — spores (LM); G — opened sporangium with sinuous, membranous columella (SEM); H, I — spores (SEM). Scale bars: A, B — 500 μm; G — 300 μm; C, D, — 200 μm, E — 50 μm, F — 10 μm, H — 5 μm, I — 1 μm.

Kedrovaya Pad Nature Reserve, flood-plain forest with *Chosenia arbutifolia* (Pall.) A.K. Skvortsov and *Phellodendron amurense* Rupr., 43.158360°N, 131.473140°E, on deciduous litter and living grass, 11 VII 2020, leg. Bortnikova N.A. and Bortnikov F.M., MYX 11357 = LE 328189 (the same colony of sporangia).

Discussion

As mentioned in the Introduction, due to the general appearance of the fruit bodies similar to those of limeless forms of *Badhamia utricularis* (Bull.) Berk., we initially assumed that the new species belonged to the genus *Badhamia* (Novozhilov et al., 2019). Indeed, *B. utricularis* also has tufts of sporangia hanging from a thread-like hypothallus. However, *B. utricularis* is otherwise strikingly different, as its peridium is often covered with lime, the capillitium is well developed, reticulate and contains many lime granules, and the spores are clustered (see Fig. 3, J in Prikhodko et al., 2023b). Phylogenetic analysis also confirms that these taxa are not related.

The species closest in micromorphology to *Diachea racemosa* is, apparently, *Diachea caespitosa* (Sturgis) Lister et G. Lister (≡ *Paradiachea caespitosa* (Sturgis) Hertel ex H. Neubert, Nowotny et K. Baumann). This species has densely clustered, caespitose sporocarps arising from a thin hypothallus, an iridescent peridium, thin pointed capillitium thread tips, and warted spores 9.6-12.8 μm in diameter, and is also associated with mosses and lichens (Sturgis, 1893). Originally, this species was described from the USA, but has since been recorded from other locations, including New Zealand and Australia (Kuhnt, 2017, Stephenson, 2021). Martin and Alexopoulos (1969), in a comment under *Comatricha caespitosa* Sturgis, additionally noted that its columella and stalk were lacking lime, and that the spores were spinulose rather than warted, with the spinules in some cases irregularly arranged. These features additionally bring *D. caespitosa* closer to *D. racemosa*.

Although the original description of *D. caespitosa* (as *Comatricha caespitosa*) has clear differences from *D. racemosa* (smaller spores, dense capillitium, and no tendency for sporangia to hang on a thread-like hypothallus), it should be noted that there are also other observations. For example, on the iNaturalist platform, the specimens of *D. caespitosa* from southern Australia and Tasmania have coarsely war-ted larger spores (about 14–15 μm) and relatively poorly developed capillitium (ID 36656817, ID 69182162) or sporangia forming tufts hanging on a whitish hypothallus (ID 140594658), and these features bring them closer to *D. racemosa* (Lloyd, 2019; McDonald, 2021; Zuidland, 2022). Unfortunately, the detailed morphological characters of these specimens and their phylogenetic position are unknown, but they apparently may represent a morphological variation of *D. caespitosa* or even a separate undescribed taxon related to *D. caespitosa* and *D. racemosa*. These specimens deserve a detailed study in the future.

According to the results of our phylogenetic analysis, previously published sequences of the two specimens of *Diachea cylindrica* Bilgram are closest to *D. racemosa* (Lado et al., 2022; García-Martín et al., 2023, monophyletic subclade 3.1 of the *Diachea* clade). However, the morphological diagnosis of *Diachea cylindrica* (≡ *Paradiachea cylindrica* (Bilgram) Hertel ex H. Neubert, Nowotny et K. Baumann), the type species of the genus *Paradiachea* Hertel, remains unresolved among researchers. Some authors consider specimens with fragile, tubular and partially or completely calcareous columella as morphological variations of *D. cylindrica* (Neubert et al., 2000; Poulain et al., 2011; Yamamoto, 2021). Two specimens of *D. cylindrica*, TVDH548 from Australia and MM46123 from Japan, are included in the phylogenetic analyses in Lado et al. (2022) and García-Martín et al. (2023). Unfortunately, the articles do not provide illustrations of these specimens, but there is a reason to believe that the specimen MM46123 is a part of the same gathering as YY-33479, since both were collected in Japan on the same day (22 VII 2012). The latter specimen, YY-33479, is illustrated by Yamamoto (2021, p. 1057) and, based on this illustration, we assign both specimens to the mentioned morphotype with a tubular fragile columella.

Bilgram, however, in the original description clearly indicated that the columella of *D. cylindrica* was completely limeless (Bilgram, 1905). Farr, who studied and illustrated a type specimen of *D. cylindrica*, also mentioned that the column was apparently always limeless (Farr, 1979). Unfortunately, it is unclear which specimen Farr illustrated, as it is labelled simply as “type”, and Bilgram also did not provide exact details of the type specimen, indicating only that it was collected in Philadelphia. Farr examined one “type” specimen and two morphologically identical specimens with

unspecified status. According to the New York Botanical Garden Herbarium website, the collection has a specimen designated as possible type: NYBG 00834220 (No. 12707, No. 465), collected by Bilgram in Philadelphia on 20 August 1899. A. Kuhnt (2017), however, also mentioned and illustrated a specimen from H. Neubert collection (M-0118732: M5419), which was also collected by Bilgram in Philadelphia, but later, in 1903. Thus, at present, there is no confirmed holotype or designated lectotype of *D. cylindrica,* but none of the authors who have seen the original material has pointed out the presence of a fragile calcareous columella in *D. cylindrica* (≡ *P. cylindrica*).

In our work, a specimen MYX 11357 collected by one of the authors (F. Bortnikov) in the Russian Far East and described in detail above was used for morphological and molecular phylogenetic comparison with *Diachea racemosa.* It has a completely limeless irregular columella and spores with coarse reticulum, which coincides with the original description of *D. cylindrica* (Bilgram, 1905).

As mentioned above, specimen MM46123, included in the phylogenetic analysis, appears to possess the morphology illustrated by Yamamoto (2021). Specimens with similar morphology were also illustrated previously by other authors, Härkönen and Saarimäki (1991, fig. 15, as *P. cylindrica*), Neubert et al. (2000, p. 251, as *P. cylindrica*), Poulain et al. (2011. Pl. 428, as *P. cylindrica*) and Kuhnt (2017, Abb. 9, Teil. 1, 2, as *P. caespitosa*). Interestingly, the same specimen from Borneo (Baumann 2533) illustrated by different authors (Neubert et al., 2000; Poulain et al., 2011; Kuhnt, 2017) is defined by them in two different ways: as *Paradiachea cylindrica* and as *P. caespitosa* (see above). At the same time, both the figure in Poulain et al. (2011) and the description in Kuhnt (2017) of this specimen make it clear that the spores of this taxon are warted and do not form a complete net, at best individual ridges and an irregular net. The same is noted in the description of a specimen from Tanzania (Härkönen and Sa-arimäki, 1991). Moreover, for specimens from Tanzania and Borneo, the authors independently reported an identical range of spore size: 9.5–14.0 μm (Härkönen and Saarimäki, 1991; Poulain et al., 2011). Unfortunately, we did not have specimens with such morphology and could not study their characters in detail to conclude on their taxonomic status.

The results of phylogenetic analysis showed that the specimens defined as *Paradiachea cylindrica* by Lado et al. (2022) and our specimen of *P. cylindrica* (which, in our opinion, in morphology is closer to the original description of Bilgram) are not related. Besides, our specimen of *P. cylindrica* falls outside the clade *Diachea* sensu lato, occupying an intermediate position between the families Lamprodermataceae and Didymiaceae. Taking into account the type status of this species, the question about the status of the genus *Paradiachea* Hertel and its composition arises again.

In our opinion, only species with truly reticulate spores and an irregular fully limeless columella should be assigned to the preserved genus *Paradiachea* sensu stricto, and species of *Paradiachea* pro parte (including *P. caespitosa* and *P. cylindrica* sensu Lado et al., 2022) with warted spores should be treated in *Diachea* sensu lato proposed by García-Martín et al. (2023). Taxonomic decisions in this direction, however, are limited by the great rarity of all *Paradiachea* species, which makes it difficult to conduct an exhaustive study involving both morphological and molecular analyses.

Our phylogenetic analysis also shows (Fig. 2) that *D. racemosa* and *D.cylindrica* sensu Lado et al. (2022) form a sister clade to the clade associated with the old genus *Scyphium* Rostaf., previously created on the basis of the type species *Craterium obovatum*, as *Scyphium rubiginosum* (Rostafiński, 1874). This clade includes *Craterium obovatum* Peck, *C. muscorum* Ing, *C. dictyosporum* (Rostaf.) H. Neubert, Nowotny et K. Baumann, and *C. lilacinum* (≡ *Badhamia lilacina*). For the latter taxon, we consider it more justified and unambiguous to use the combination within the genus *Craterium* (*C. lilacinum*), which was proposed by Massee (1892) already more than 130 years ago based on morphological characters. He suggested, "The present species may eventually prove to be a sessile form of *C. dictyospermum*", now *C. dictyospermum* Massee is a synonym of *C. obovatum*. In our opinion, all these species should be transferred to the genus *Scyphium* based of the phylogenetic analysis and morphological resemblance (Massee, 1892). In addition, we see a contradictory position of the morphological species *Diderma cor-rubrum* in our phylogenetic tree (Fig. 2). Regardless of which genes we selected for the analysis, this species always grouped with species of the genus *Diachea* sensu stricto corresponding to the subclade 3-II of the clade 3 "*Diachea*" in the phylogenetic tree of Physarales (García-Martín et al., 2023).

As mentioned in the Introduction, sequences of the type specimen of *Diachea racemosa* were erro-

neously submitted to Genbank under the name *Badhamia lilacina* (Shchepin et al., 2021) and were subsequently used under this name in the phylogenetic analysis of the order Physarales (García-Martín et al., 2023). To correct these errors, we used in our phylogenetic analysis several specimens of *Craterium lilacinum* (≡ *B. lilacina*) from different regions of the European Russia. The morphological description and illustrations of *C. lilacinum*, which we have given above, correspond to the morphological concept of this species and other descriptions published earlier (Massee, 1892; Martin and Alexopoulos, 1969; Hatano and Keller, 2008). It is worth noting that in the peridium, capillitium, and stalk-like base of *C. lilacinum* we found only lime granules (Fig. 3, G), but not large prismatic or rhombohedral crystals noted earlier for *Diachea* sensu lato species (Keller et al., 2004; Cavalcanti et al., 2009) and which we found in the stalks of *Craterium dictyosporum* (≡ *Diachea dictyospora* (Rostaf.) J.M. García-Martín, J.C. Zamora et Lado) (Fig. 3, H). This may suggest limitations in the application of this feature for generic delimitations, but a final decision on this issue requires a special study using SEM.

Therefore, we plan to resurrect the genus *Scyphium* and clarify the taxonomic status of the genera *Diachea* sensu lato and *Paradiachea* sensu lato in a future study using additional materials and data.

Acknowledgements

DNA extraction, low-pass genome sequencing of myxomycetes and bioinformatic analysis of the data were fully supported financially by the Russian Science Foundation (project No. 22-24-00747; https://rscf.ru/project/22-24-00747/). We acknowledge the use of equipment of the Core Facility Center "Cell and Molecular Technologies in Plant Science" at the Komarov Botanical Institute of the Russian Academy of Sciences (BIN RAS, St. Petersburg) and send personal thanks to Lyudmila Kartzeva, lead engineers of the Core Facility Center, and to the staff of the Joint Russian-Vietnamese Tropical Research and Technological Centre for organization of the field work in the frame of the program "Ecolan 1.5". We also thank the staff of the Interdepartmental Laboratory of Electron Microscopy (ILEM) at the Faculty of Biology of Moscow State University, where high-resolution SEM images of some specimens were obtained.

References

Bilgram H. 1905. *Diachea cylindrica*, a new species of Mycetozoa. P. Acad. Nat. Sci. Philadelphia. 57: 524.

Bortnikov F.M., Bortnikova N.A., Gmoshinskiy V.I., Prikhodko I.S. and Novozhilov Y.K. 2023. Additions to *Trichia botrytis* complex (Myxomycetes): 9 new species. Bot. Pacifica. 12 (2): 81–119 https://doi.org/10.17581/bp.2023.12s03

Cavalcanti L.H., Bezerra A.C.C., Costa A.A.A., Ferreira I.N. and Bezerra M.F.A. 2009. Distribution of *Diachea* (Didymiaceae, Myxomycetes) in the northeastern region of Brazil. Mycotaxon. 110: 163–172. https://doi.org/10.5248/110.163

Farr M.L. 1979. Notes on Myxomycetes II. New taxa and records. Nova Hedwigia. 31: 103–118.

Feng Y. and Schnittler M. 2015. Sex or no sex? Group I introns and independent marker genes reveal the existence of three sexual but reproductively isolated biospecies in *Trichia varia* (Myxomycetes). Org. Divers. Evol. 15 (4): 631–650. https://doi.org/10.1007/s13127-015-0230-x

Fiore-Donno A.M., Berney C., Pawlowski J. and Baldauf S. 2005. Higher-Order phylogeny of plasmodial slime molds (Myxogastria) based on elongation factor 1-A and small subunit rRNA gene sequences. J. Eukaryot. Microbiol. 52 (3): 201–210. https://doi.org/10.1111/j.1550-7408.2005.00032.x

Fiore-Donno A.M., Meyer M., Baldauf S.L. and Pawlowski J. 2008. Evolution of dark-spored Myxomycetes (slime-molds): molecules versus morphology. Mol. Phylogenetics Evol. 46 (3): 878–889. https://doi.org/10.1016/j.ympev.2007.12.011

Fiore-Donno A.M., Nikolaev S.I., Nelson M., Pawlowski J. et al. 2010. Deep phylogeny and evolution of slime moulds (Mycetozoa). Protist. 161 (1): 55–70. https://doi.org/10.1016/j.protis.2009.05.002

Fiore-Donno A.M., Tice A.K. and Brown M.W. 2019. A non-flagellated member of the Myxogastria and expansion of the Echinosteliida. J. Eukaryot. Microbiol. 66 (4): 538–544. https://doi.org/10.1111/jeu.12694

García-Martín J.M., Zamora J.C., Lado C. 2023.Multigene phylogeny of the order Physarales (Myxomycetes, Amoebozoa): Shedding light on the dark-spored clade. Persoonia. 51: 89–124. https://doi.org/10.3767/persoonia.2023.51.02

Härkönen M. and Saarimäki T. 1991 Tanzanian Myxomycetes: first survey. Karstenia. 31 (2): 31–54. https://doi.org/10.29203/ka.1991.284

Hatano T. and Keller H.W. 2008. Spore ornamentations of selected *Badhamia* species using a scanning electron microscopy. Bull. Shitennoji Univ 47: 113–122.

Hoang D.T., Chernomor O., von Haeseler A., Minh B.Q. and Vinh L.S. 2018. UFBoot2: Improving the ultrafast bootstrap approximation. Mol. Biol. Evol. 35 (2): 518–522. https://doi.org/10.1093/molbev/msx281

Huelsenbeck J.P. and Ronquist F. 2001. MR BAYES: Bayesian inference of phylogenetic trees. Bioinformatics. 17 (8): 754–755. https://doi.org/10.1093/bioinformatics/17.8.754

Ing B. 1994. The phytosociology of Myxomycetes. New Phytol. 126: 175–201. https://doi.org/10.1111/j.1469-8137.1994.tb03937.x

Kalyaanamoorthy S., Minh B.Q., Wong T.K.F., von Haeseler A. and Jermiin L.S. 2017. ModelFinder: fast model selection for accurate phylogenetic estimates. Nat. Methods. 14: 587–589. https://doi.org/10.1038/nmeth.4285

Katoh K. and Standley D.M. 2013. MAFFT multiple sequence alignment software version 7: improvements in performance and usability. Mol. Biol. Evol. 30 (4): 772–780. https://doi.org/10.1093/molbev/mst010

Katoh K., Rozewicki J. and Yamada K.D. 2019. MAFFT online service: multiple sequence alignment, interactive sequence choice and visualization. Brief. Bioinform. 20 (4): 1160–1166. https://doi.org/10.1093/bib/bbx108

Keller H.W., Skrabal M., Eliasson U.H. and Gaither T.W. 2004. Tree canopy biodiversity in the Great Smoky Mountains National Park: ecological and developmental observations of a new myxomycete species of *Diachea*. Mycologia. 96 (3): 537–547. https://doi.org/10.1080/15572536.2005.11832952

Kuhnt A. 2017. Bemerkenswerte Myxomycetenfunde: Neue Arten, Neukombinationen und Nachweise seltener Arten. Ber. Bayer. Bot. Ges. 87: 93–128 (in German).

Lado C. 2005–2023. An on-line nomenclatural information system of Eumycetozoa. Available online at: http://www.eumycetozoa.com (accessed on 16 VII 2023).

Lado C., Trevico-Zevallos I., García-Martín J.M. and Wrigley de Basanta D. 2022. *Diachea mitchellii*: a new myxomycete species from high elevation forests in the tropical Andes of Peru. Mycologia. 114 (4): 798–811. https://doi.org/10.1080/00275514.2022.2072140

Leontyev D.V., Schnittler M., Stephenson S.L., Novozhilov Y.K. and Shchepin O.N. 2019. Towards a phylogenetic classification of the Myxomycetes. Phytotaxa. 399 (3): 209–238. https://doi.org/10.11646/phytotaxa.399.3.5

Lloyd S. 2019. https://www.inaturalist.org/observations/36656817 (accessed on 25 X 2023)

Martin G.W. and Alexopoulos C.J. 1969. The Myxomycetes. University of Iowa Press, Iowa City.

Massee G. 1892. Monograph of the Myxogastres. Methuen, London. https://doi.org/10.5962/bhl.title.31927

McDonald P. 2021. https://www.inaturalist.org/observations/69182162 (accessed on 25 X 2023)

Mikheenko A., Prjibelski A., Saveliev V., Antipov D. and Gurevich A. 2018. Versatile genome assembly evaluation with QUAST-LG. Bioinformatics. 34 (13): i142–i150. https://doi.org/10.1093/bioinformatics/bty266

Miller M.A., Pfeiffer W. and Schwartz T. 2010. Creating the CIPRES Science Gateway for inference of large phylogenetic trees. 2010 Gateway Computing Environments Workshop (GCE), New Orleans, pp. 1–8. https://doi.org/10.1109/GCE.2010.5676129

Neubert H., Nowotny W., Baumann K. 2000. Die Myxomyceten Deutschlands und des angrenzenden Alpenraumes unter besonderer Berücksichtigung Österreichs: Stemonitales Band 3. Stemonitales. Karlheinz Baumann Verlag, Gomaringen (in German).

Nguyen L.T., Schmidt H.A., von Haeseler A. and Minh B.Q. 2015. IQ-TREE: a fast and effective stochastic algorithm for estimating maximum-likelihood phylogenies. Mol. Biol. Evol. 32 (1): 268–274. https://doi.org/10.1093/molbev/msu300

Novozhilov Y.K., Okun M.V., Erastova D.A., Shchepin O.N. et al. 2013. Description, culture and phylogenetic position of a new xerotolerant species of *Physarum*. Mycologia. 105 (6): 1535–1546. https://doi.org/10.3852/12-284

Novozhilov Y.K., Prikhodko I.S. and Shchepin O.N. 2019. A new species of *Diderma* from Bidoup Nui Ba National Park (southern Vietnam). Protistology. 13 (3):126–132. doi:10.21685/1680-0826-2019-13-3-2

Novozhilov Y.K., Shchepin O.N., Schnittler M., Dagamac N.H.A. et al. 2020. Myxomycetes associated with mountain tropical forests of Bidoup Nui Ba and Chu Yang Sin national parks (Dalat Plateau, southern Vietnam). Nova Hedwigia. 110 (1–2): 185–224. https://doi.org/10.1127/nova_hedwigia/2019/0560

Novozhilov Y.K., Prikhodko I.S., Fedorova N.A., Shchepin O.N. et al. 2022. *Lamproderma*

vietnamense: a new species of myxomycetes with reticulate spores from Phia Oắc – Phia Pén National Park (northern Vietnam) supported by molecular phylogeny and morphological analysis. Mycoscience. 63 (4): MYC577. https://doi.org/10.47371/mycosci.2022.05.003

Okonechnikov K., Golosova O., Fursov M. and UGENE team. 2012. Unipro UGENE: a unified bioinformatics toolkit. Bioinformatics. 28: 1166–1167. https://doi.org/10.1093/bioinformatics/bts091

Poulain M., Meyer M. and Bozonnet J. 2011. Les Myxomycetes. Fédération mycologique et botanique Dauphiné-Savoie, Sévrier.

Prikhodko I.S., Shchepin O.N., Bortnikova N.A., Novozhilov Y.K. et al. 2023a. A three-gene phylogeny supports taxonomic rearrangements in the family Didymiaceae (Myxomycetes). Mycol. Progr. 22 (2): 11. https://doi.org/10.1007/s11557-022-01858-1

Prikhodko I.S., Shchepin O.N., Novozhilov Y.K., Gmoshinskiy V.I. and Schnittler M. 2023b. Reassessing the phylogenetic position of the genus *Kelleromyxa* (Myxomycetes = Myxogastrea) using genome skimming data. Protistology. 17 (2): 73–84. https://doi.org/10.21685/1680-0826-2023-17-2-2

Prjibelski A., Antipov D., Meleshko D., Lapidus A. and Korobeynikov A. 2020. Using SPAdes de novo assembler. Curr. Protoc. Bioinform. 70: e102. https://doi.org/10.1002/cpbi.102

Rambaut A., Drummond A.J., Xie D., Baele G. and Suchard M.A. 2018. Posterior summarization in Bayesian phylogenetics using Tracer 1.7. Syst. Biol. 67 (5): 901–904. https://doi.org/10.1093/sysbio/syy032

Ronikier A., García-Cunchillos I., Janik P. and Lado C. 2020. Nivicolous Trichiales from the austral Andes: unexpected diversity including two new species. Mycologia. 112 (4): 753–780. https://doi.org/10.1080/00275514.2020.1759978

Rostafiński J. 1874. Śluzowce (Mycetozoa). Pamiętnik Towarzystwa Nauk Ścisłych w Paryżu 5.

Shchepin O., Novozhilov Y., Woyzichovski J., Bog M. et al. 2021. Genetic structure of the protist *Physarum albescens* (Amoebozoa) revealed by multiple markers and genotyping by sequencing. Molec. Ecol. 31: 372–390. https://doi.org/10.1111/mec.16239

Stephenson S.L. 2021. Secretive Slime Moulds: Myxomycetes of Australia. CSIRO Publishing, Canberra.

Sturgis W.C. 1893. On two new or imperfectly known Myxomycetes. Bot. Gaz. 18 (5): 186–87.

Vaidya G., Lohman D.J. and Meier R. 2011. SequenceMatrix: concatenation software for the fast assembly of multi-gene datasets with character set and codon information. Cladistics. 27: 171–180. https://doi.org/10.1111/j.1096-0031.2010.00329.x

Wrigley de Basanta D., Estrada-Torres A., García-Cunchillos I., Cano Echevarria A. and Lado C. 2017. *Didymium azorellae*, a new myxomycete from cushion plants of cold arid areas of South America. Mycologia. 109 (6): 993–1002. https://doi.org/10.1080/00275514.2018.1426925

Yamamoto Y. 2021. Biota of Japanese Myxomycetes. Committee for the publication of Biota of Japanese Myxomycetes, Ibaraki (in Japan).

Zuidland P. 2022. https://www.inaturalist.org/observations/140594658 (accessed on 25 X 2023)

Supplementary material

File S1. Concatenated alignment.

File S2. Partition file in RAxML format.

Table S1. List of sequences used in this study.

The list of sequences obtained in this study, the concatenated alignment, partition file, and raw phylogenetic tree can also be found in FigShare (https://doi.org/10.6084/m9.figshare.24591222).